

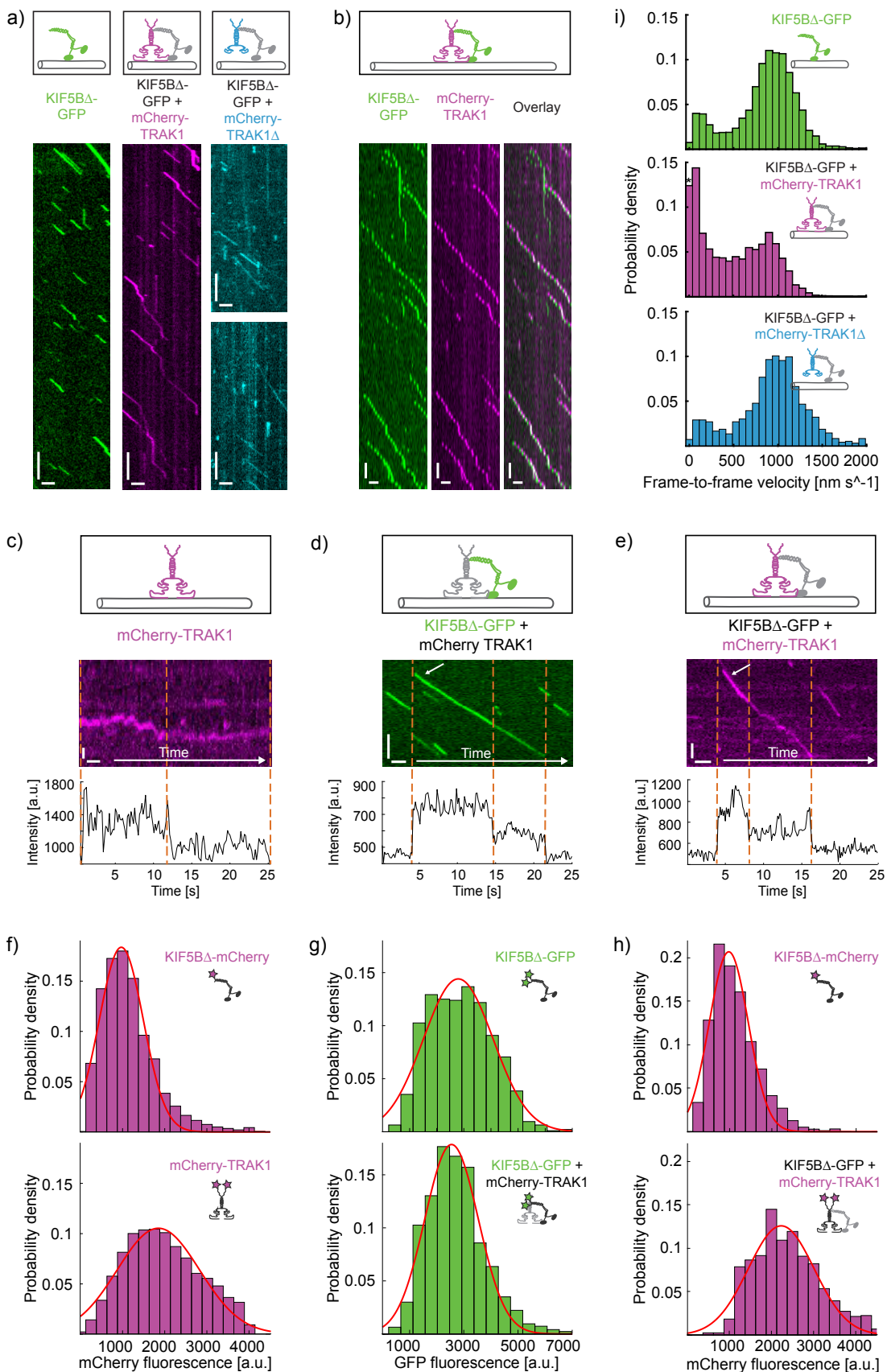
Supplementary Information

**Mitochondria-adaptor TRAK1 promotes kinesin-1 driven transport
in crowded environments**

Henrichs et al.



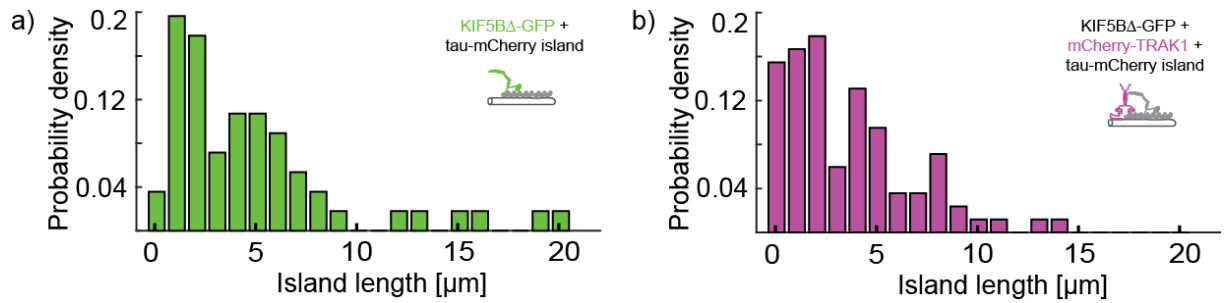
Supplementary Figure 1. Related to Figure 1-5. **a)** List of constructs used in this study. The asterisk indicates the position of the T93N point mutation of the rigor binding kinesin-1 mutant rkin430. **b)** SDS-gel of purified mCherry-TRAK1. **c)** SDS-gel of purified mCherry-TRAK1 Δ . Source data are provided as a Source Data file.



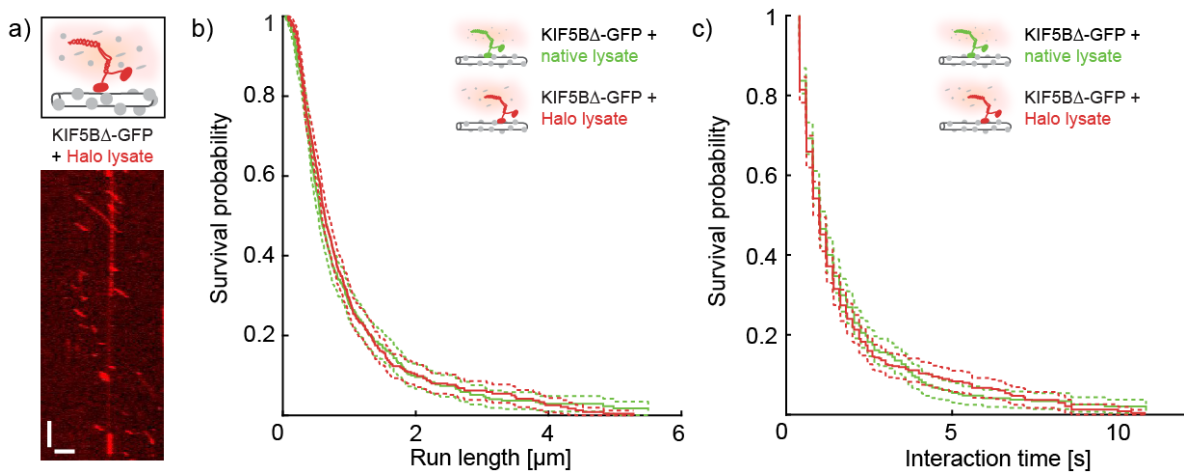
Supplementary Figure 2. Related to Figure 2 and 5. **a)** Schematic illustrations and kymographs of processively moving KIF5B Δ -GFP (green), mCherry-TRAK1 in presence of KIF5B Δ -GFP (magenta) and mCherry-TRAK1 Δ in presence of KIF5B Δ -

GFP (cyan). Horizontal scale bars 2 μ m, vertical 5 s. **b)** Schematic illustration and kymographs of KIF5B Δ -GFP colocalizing with mCherry-TRAK1 and walking processively along a microtubule. Horizontal scale bars 2 μ m, vertical 5 s. **c) - e)** Schematic illustrations, kymographs and intensity time traces (Methods) showing two-step photobleaching of the mCherry signal of mCherry-TRAK1 diffusing along a microtubule and of the GFP and mCherry signal, respectively, of KIF5B Δ -GFP-mCherry-TRAK1 complexes walking processively along a microtubule, suggesting the presence of both molecules in a dimeric form. The white arrows indicate the molecules yielding the respective time traces. The dashed lines indicate the photobleaching steps. Horizontal scale bars 2 s, vertical 1 μ m. **f)** Histograms of the background-subtracted integrated fluorescence intensities of the mCherry signal and Gaussian fits (red) of constitutively dimeric^{31,77} KIF5B Δ -mCherry (top, $n = 355$ molecules) and of mCherry-TRAK1 (bottom, $n = 256$ molecules). Size exclusion chromatography measurements revealed that the large majority of KIF5B Δ -mCherry dimers harbor a single active mCherry fluorophore, while the large majority of mCherry-TRAK1 dimers harbor two active mCherry fluorophores (Methods, Supplementary Table 1). We thus interpret the single peak in the KIF5B Δ -mCherry intensity distribution as the signal of a single active mCherry fluorophore harbored by the (constitutively dimeric) KIF5B Δ and the single peak in the mCherry-TRAK1 distribution (centered at around twice the KIF5B Δ -mCherry intensity) as the signal of two active mCherry fluorophores harbored by a TRAK1 dimer. **g)** Histograms of the background-subtracted integrated fluorescence intensities of the GFP signal and Gaussian fits (red) of the constitutively dimeric KIF5B Δ -GFP (top, $n = 79$ molecules) and KIF5B Δ -GFP in complex with mCherry-TRAK1 (bottom, $n = 150$ molecules). The similar position of the peaks in both histograms indicates that a single KIF5B Δ -GFP dimer is present in a KIF5B Δ -GFP-mCherry-TRAK1 transport complex. **h)** Histograms of the background-subtracted integrated fluorescence intensities of the mCherry signal and Gaussian fits (red) of KIF5B Δ -mCherry (top, $n = 33$ molecules) harboring a single mCherry fluorophore per dimer (Methods, Supplementary Table 1) and mCherry-TRAK1 harboring two mCherry fluorophores per dimer (Methods, Supplementary Table 1) in complex with KIF5B Δ -GFP (bottom, $n = 150$ molecules). Analogously to f), the position of the peak in the histogram of mCherry-TRAK1 in complex with KIF5B Δ -GFP (centered at around twice the KIF5B Δ -mCherry intensity) indicates that a single TRAK1 dimer is present in a KIF5B Δ -GFP-mCherry-TRAK1 transport complex. **i) c)** Histograms of frame-to-frame

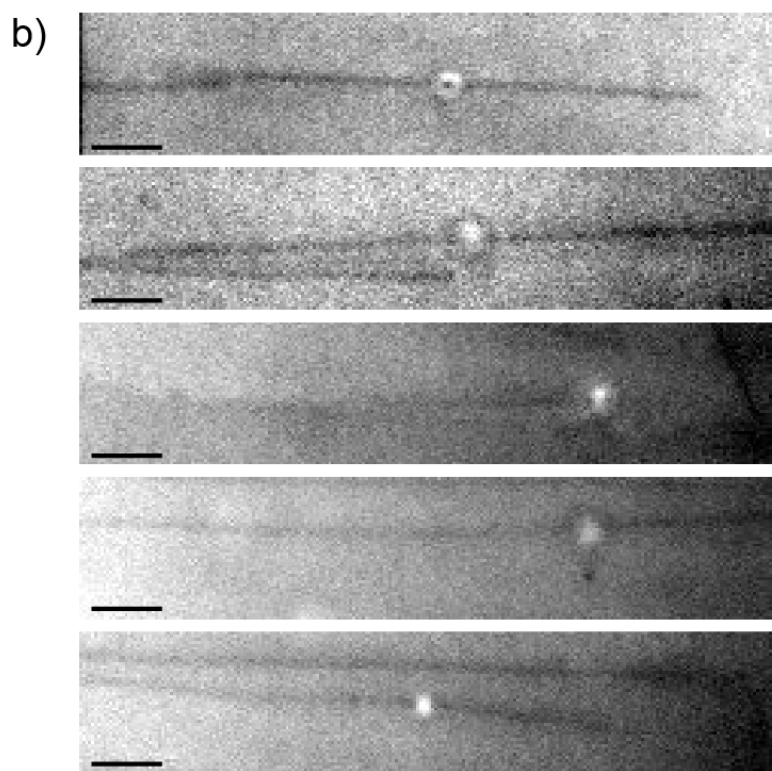
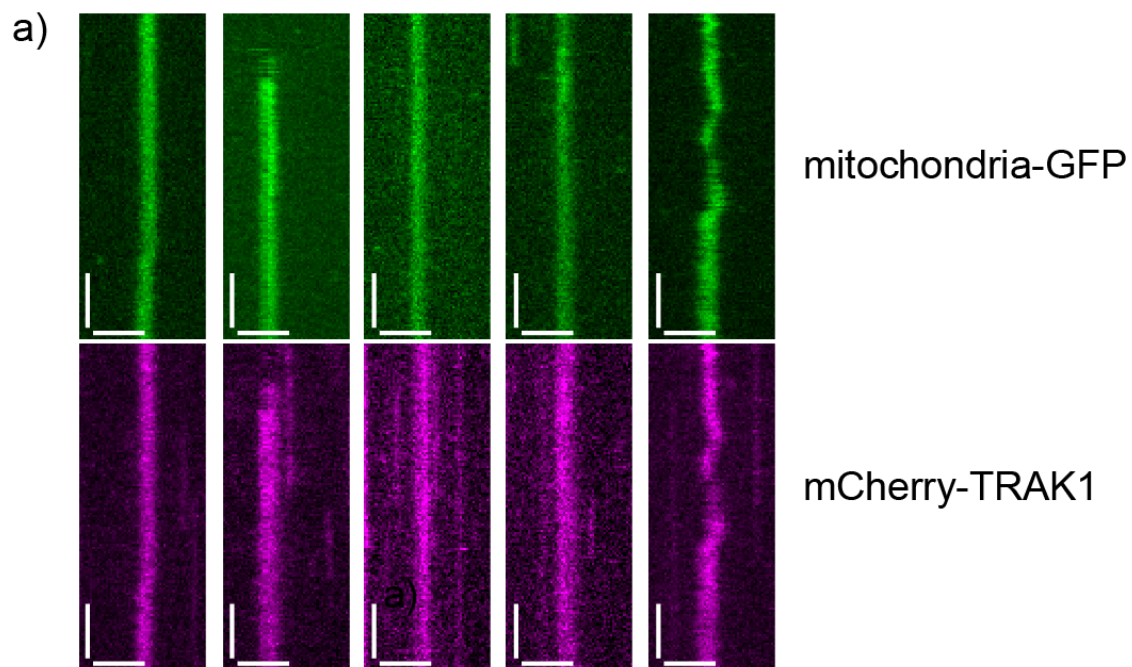
velocities of KIF5BΔ-GFP (green), KIF5BΔ-GFP in presence of mCherry-TRAK1 (magenta) and KIF5BΔ-GFP in presence of mCherry-TRAK1 Δ (cyan). The median frame-to-frame velocity of KIF5BΔ-GFP decreased in presence of mCherry-TRAK1 from 909 nm s $^{-1}$ (lower, upper quantile limit 687 nm s $^{-1}$, 1085 nm s $^{-1}$, $n = 534$ molecules, $N = 2$ experiments) to 458 nm s $^{-1}$ (lower, upper quantile limit 97 nm s $^{-1}$, 842 nm s $^{-1}$, $n = 487$ molecules, $N = 4$ experiments). The population around zero (indicated by an asterisk) represents a high number of transient pauses. In presence of mCherry-TRAK1 Δ the median frame-to-frame velocity of KIF5BΔ-GFP did not decrease (972 nm s $^{-1}$, lower, upper interquartile limit 732 nm s $^{-1}$, 1060 nm s $^{-1}$, $n = 82$ molecules, $N = 2$ experiments). Experiments were repeated at least 10 times with similar results. Source data are provided as a Source Data file.



Supplementary Figure 3. Related to Figure 3. Histograms of the tau island length distribution in experiments with **a)** KIF5B Δ -GFP ($4.75 \pm 4.8 \mu\text{m}$, mean \pm standard deviation, $n = 56$ islands, $N = 4$ experiments) and **b)** KIF5B Δ -GFP-mCherry-TRAK1 complexes ($3.54 \pm 3.12 \mu\text{m}$, mean \pm standard deviation, $n = 84$ islands, $N = 4$ experiments). Source data are provided as a Source Data file.



Supplementary Figure 4. Related to Figure 4. **a)** Schematic illustration and kymograph of processively moving KIF5B Δ -GFP in Halo lysate. Horizontal scale bar 1 μm , vertical 10 s. **b), c)** Survival probabilities indicating a similar median run length (0.63 μm (CI_{95} (0.58, 0.69) μm , $n = 555$ molecules, $N = 6$ experiments)) and interaction time (1 s (CI_{95} (0.82, 1.02) s, $n = 555$ molecules, $N = 6$ experiments)) of KIF5B Δ -GFP in Halo lysate (red) in comparison to native lysate (green) (compare to Figure 4h,i) ($p = 0.6$ and $p = 0.3$, respectively). Two-tailed p -values were obtained by a log-rank test. Source data are provided as a Source Data file.



Supplementary Figure 5. Related to Figure 5. a) Kymographs showing stationary and diffusive tethering of mitochondria-GFP (green) to microtubules by mCherry-TRAK1 (magenta). The experiment was repeated 5 times independently with similar results). Horizontal scale bars 2 μ m, vertical 10 s. **b)** Representative interference reflection microscopy images of single mitochondria bound to microtubules. Scale bars 2 μ m.

Supplementary Table 1: Values for calculating the labelling efficiencies of KIF5B Δ -mCherry and mCherry-TRAK1

	KIF5B Δ -GFP	mCherry-TRAK1
Absorbance at 280 nm [AU] (A_{280})	35.96	44.00
Absorbance at 561 nm [AU] (A_{561})	6.85	33.95
Extinction coeff. of protein at 280 nm [$M^{-1} cm^{-1}$] (\mathcal{E}_{280})	82500	82000
Extinction coeff. of protein at 561 nm [$M^{-1} cm^{-1}$] (\mathcal{E}_{561})	72000	72000
Labelling efficiency	0.2183	0.8787

A is the absorbance and \mathcal{E} the extinction coefficient at 280 nm (A_{280} and \mathcal{E}_{280}) and 561 nm (A_{561} and \mathcal{E}_{561}), respectively.

Supplementary Table 2: Primers used in this work.

	Forward primers	Reverse primer	PCR
mCherry- TRAK1	TCGGAGAACCTGTACTTC CAGTCTACCATGGTGAGC AAGGGCGAGGAGGATAAC ATG	GGGGACCACTTGTACAAGAA AGCTGGTTATTACCGTAAGCT AGTTTGTGGAGAG	Gateway step 1
mCherry- TRAK1	GGGGACAAGTTGTACAA AAAAGCAGGCTCGGAGAA CCTGTACTTCCAG	GGGGACCACTTGTACAAGAA AGCTGGTTATTACCGTAAGCT AGTTTGTGGAGAG	Gateway step 2
mCherry- TRAK1Δ	GACACAGGTGACCACTAA ATTCTCTCCCACGC	GCGTGGGAGAGAAATTAGTG GTCACCTGTGTC	Mutagenesis
KIF5B	AATAATAACATGCGGCCG CAATGGCGGACCTGGCCG AGTG	AATAATAACATGGCGCGCCCA CTTGTGGCCTCCTCCACCTC	Amplification
KIF5BΔ	AATAATAACATGCGGCCG CAATGGCGGACCTGGCCG AGTG	AATAATAACATGGCGCGCTG CTTCCTTATGCGATCTACTTC TTGC	Amplification